J Exp Biol Advance Online Articles. First posted online on 2 September 2016 as doi:10.1242/jeb.134775
Access the most recent version at http://jeb.biologists.org/lookup/doi/10.1242/jeb.134775

Assessing hydrodynamic space use of brown trout, *Salmo trutta*, in a complex flow environment: A return to first principles

James R Kerr[a], Costantino Manes[a,b], and Paul S. Kemp[a*]*

a: International Centre for Ecohydraulics Research, Faculty of Engineering and the Environment, University of Southampton, Highfield, Southampton, SO17 1BJ, UK.

b:Department of Environment, Land and Infrastructure Engineering, Politecnico di Torino, Corso Duca degli Abruzzi, 24, 10129, Torino, Italy.

∗ Corresponding authors. Tel.: +44 0 2380 595871

E-mail addresses: j.r.kerr@soton.ac.uk (Kerr, J.R.), p.kemp@soton.ac.uk (Kemp, P.S.).

Keywords: Energetics, behaviour, cylinders, drag, turbulence, trout.

Summary Statement

New techniques are used to experimentally demonstrate that energy conservation strategies play a key role in brown trout space use.

List of symbols and abbreviations

Notation	*Unit*	*Description*
u	m s^{-1}	longitudinal velocity component
v	m s^{-1}	Lateral velocity component
w	m s^{-1}	Vertical velocity component
U	m s^{-1}	Mean three dimensional velocity magnitude
σ	m s^{-1}	Standard deviation (i.e. σ_v lateral velocity standard deviation)
U_f	m s^{-1}	Cross-section mean velocity (measured 500 mm downstream of the flow straightener)
St	N/A	Strouhal number (0.2, appropriate for the range of Reynolds numbers in this experiment - Sumer and Fredsøe, 1997)
W	m	Width of the flume
ρ	kg m^{-3}	Density (1000 kg m^{-3})

t	s	Time
τ	s	Time lag
TI	m s^{-1}	Turbulence intensity
TI_R	N/A	Relative turbulence intensity
TKE	J m^{-3}	Turbulent kinetic energy
TLS	m	Turbulent length scale
τ_{uw}	N m^{-2}	Horizontal Reynolds shear stress
D	N/A	Drag (including the influence of turbulent fluctuations)
N	Count	Number of fish
R_e	N/A	Reynolds number
f	Hz	Vortex shedding frequency
λ	m	Wake wavelength
E_s	m s^{-1}	Convection speed of the dominant energy containing eddies
E_t	s	Turnover time of the dominant energy containing eddies
E_d	m	Characteristic size of the dominant energy containing eddies
C_d	N/A	Dimensionless drag coefficient
S	m^2	Form area
H_p	N/A	Hydrodynamic preference
S_u	N/A	Space used
S_s	N/A	Space sampled
GH_p	N/A	Group hydrodynamic preference
H_t	N/a	Total available hydrodynamic space
TD	s	Trial duration

Abstract

It is commonly assumed that stream-dwelling fish should select positions where they can reduce energetic costs relative to benefits gained and enhance fitness. However, the selection of appropriate hydrodynamic metrics that predict space use is the subject of recent debate and a cause of controversy. This is for three reasons: 1) flow characteristics are often oversimplified, 2) confounding variables are not always controlled, and 3) there is limited understanding of the explanatory mechanisms that underpin the biophysical interactions between fish and their hydrodynamic environment. This study investigated the space use of brown trout, *Salmo trutta*, in a complex hydrodynamic flow field created using an array of different sized vertically oriented cylinders in a large open-channel flume in which confounding variables were controlled. A hydrodynamic drag function based on single-point time-averaged velocity statistics that incorporates the influence of turbulent fluctuations (*D*) was used to infer the energetic cost of steady swimming. Novel hydrodynamic preference curves were developed and used to assess the appropriateness of *D* as a descriptor of space use compared to other commonly used metrics. Zones in which performance enhancing swimming behaviours (e.g. Kármán gaiting, entraining, and bow riding) that enable fish to hold position while reducing energetic costs (termed 'specialised behaviours') were identified and occupancy recorded. We demonstrate that energy conservation strategies play a key role in space use in an energetically taxing environment with the majority of trout groups choosing to frequently occupy areas where specialised behaviours may be adopted or by selecting low drag regions.

Journal of Experimental Biology • Advance article

1. Introduction

Understanding how the physical environment influences the distribution and movement of animals is a fundamental theme in ecology (Moorcroft, 2012). To maximise fitness, individuals must utilise space in ways that facilitates energy intake, through the acquisition of food, while minimising costs (Krebs, 1978; Maynard Smith, 1978). Those that most effectively do so can allocate a greater proportion of available resources (time and energy) to other activities, such as the detection and evasion of predators, growth, and reproduction (Parker and Maynard Smith, 1990). For stream dwelling fish adapted to the challenges imposed by a spatially and temporally complex hydrodynamic environment, energetic costs include those associated with maintaining stability (Tritico and Cotel, 2010; Webb and Cotel, 2011), swimming (Enders *et al.,* 2003; Liao, 2004) and capturing food (Chesney, 1989). The use of space that enables fish to minimise energy expenditure under complex flows is of interest to evolutionary biologists, ecologists, fisheries managers and conservationists, and is the focus of this study.

The selection of appropriate hydrodynamic metrics that predict space use by fish has been the subject of recent debate (Lacey *et al.* 2012) and a cause of controversy. This is for three reasons. First, traditional methods tend to heavily rely on the correlation between single-point time-averaged velocity statistics with space use by fish (e.g. Bovee, 1986; DeGraaf & Bain, 1986; Facey and Grossman, 1992; Mäki-Petäys *et al*., 1997; Jenkins and Keeley, 2010). Such measures fail to capture important flow-fish interaction mechanisms that rely on turbulent flow properties that vary both in time and space. For example, fish use spatial flow patterns around bluff bodies to hold position with reduced energy expenditure by tilting their body at an angle where hydrodynamic forces cancel out (e.g. entraining - Przybilla *et al.,* 2010). Second, attempts to quantify habitat use by fish in the field typically produce mixed results (e.g. Heggenes *et al.,* 1991; Facey and Grossman, 1992; Jowett and Richardson, 1995; Mäki-Petäys *et al*., 1997; Cotel *et al.,* 2006; Enders *et al.,* 2009). This is not surprising because space use is influenced by multiple confounding variables impossible to control *in situ* (e.g. food, predators, competitors, and mates). Third, laboratory studies continue to attempt to find statistical links between patterns of fish distribution/movement and one or more of any number of turbulent flow characteristics, such as turbulence intensity (*TI*), relative turbulence intensity (TI_R), turbulent kinetic energy (*TKE*), turbulent length scale (*TLS*), or Reynolds shear stresses (τ) (e.g. Smith *et al.,* 2005; 2006; Silva *et al.*, 2011; 2012a; 2012b; Duarte *et al.,* 2012). However, the biophysical interpretation of these statistical links remains obscure. This results in the failure to understand and investigate the explanatory mechanisms that underpin interactions between fish and their

hydrodynamic environment. There is a need to return to first principles and quantify space use by fish in response to complex flows under controlled laboratory conditions. Furthermore, experimental data must be interpreted in-line with the general principle that space use is dictated by energy conservation, or more specifically, strategies to minimise the costs of swimming.

The energetic cost of swimming for motile organisms is intrinsically linked to drag and mass-related gravitational forces (Biewener *et al*., 2003). For fish, which are typically of a similar density to the surrounding medium, hydrodynamic drag imposes the largest influence on locomotion because mass-related gravitational forces are negligible (Biewener *et al*., 2003). As such, the reduction of hydrodynamic drag plays an important role in improving swimming performance. Fish have evolved numerous passive and active mechanisms to reduce drag and hence energetic costs during locomotion. For example, the streamlined morphology of a fish reduces flow separation and minimises form drag (Vogel, 1996), while epidermal mucus (Daniel, 1981) and riblets (Dean and Bhushan, 2010) reduce skin friction (passive mechanisms). In addition, conventional swimming kinematics are optimised to prevent flow separation during undulation (Anderson *et al.,* 2001), fish can take advantage of reduced drag during intermittent non-undulatory phases of burst-glide locomotion (Weihs, 1974), and, as already mentioned, they can use stable or predictable flow characteristics around bluff bodies to hold position whilst reducing energetic expenditure (Taguchi and Liao, 2011) (active mechanisms). Even when fish exhibit behaviours where other fundamental biological needs are of primary importance these are undertaken in a way whereby energy expenditure is minimised (e.g. feeding: Fausch, 1984; reproductive migration: McElroy *et al.,* 2012). As such, energy minimising strategies play a fundamental role in fish ecology and hence are likely to be an important driver in space use. However, calculating the drag force acting on a fish at a specific hydrodynamic location, and hence investigating the link between space use and energy expenditure, is difficult because sources of thrust and drag are not separable for undulating swimmers (Schultz and Webb, 2002). Although advances are being made in assessing the energetic costs and efficiency of swimming (e.g. Maertens *et al.,* 2014), there are still few viable options for accurately calculating likely energetic expenditure at specific hydrodynamic locations.

This study adopted a reductionist approach to investigate hydrodynamic space use by brown trout, *Salmo trutta* (Linnaeus, 1758), under a controlled experimental setting in which key confounding variables (e.g. visual cues, food, predators and conspecifics) were absent. The term 'hydrodynamic space use' is used to refer to the distribution of an animal in space in relation to local flow characteristics. To facilitate generalisation of the results, trout from both wild and hatchery origin

exhibiting a range of body lengths were used. The position of individual fish was recorded at high spatial resolution in a complex flow field created using an array of different sized vertically oriented cylinders in a large open-channel flume. The flow field offered a highly heterogeneous hydrodynamic environment and consequently a wide range of potential positions from which the fish could choose. We hypothesise that under the conditions presented, space use would be governed by the adoption of energy conservation strategies. A hydrodynamic drag function (*D*) based on single-point time-averaged velocity statistics that incorporates the influence of turbulent fluctuations was used to infer the energetic cost of steady swimming. Further, zones in which there was a potential for fish to exhibit 'specialised behaviours' that rely on spatial and/or temporal flow features and enable fish to hold position with reduced energetic cost (e.g. Kármán gaiting, entraining, and bow riding) were identified and their occupancy recorded. Preference curves were constructed to assess the appropriateness of *D* as a descriptor of space use in comparison to other common hydrodynamic metrics: mean velocity (*U*), *TI*, TI_R, *TKE*, horizontal Reynolds shear stress (τ_{uv}), and *TLS*. A fundamental assumption and potential source of error of conventional methods of calculating preference (use-versus-availability) is that an organism has access to, and knowledge of, all space available to them (Beyer *et al.,* 2010). In this study preference calculations were refined by assessing space use of individual fish in relation to area 'sampled' rather than total available. The results of this study, and the methods presented, have important implications for the understanding of the ecology of fluvial fish that live in hydrodynamically complex environments, and for fisheries management and conservation.

2. Methodology

2.1. Experimental setup

The study was conducted in a large indoor recirculating flume (21.4 m long, 1.4 m wide, and 0.6 m deep) at the International Centre for Ecohydraulics Research (ICER) facility, University of Southampton, UK (50° 57'42.6"N, 1°25'26.9"W). The experimental area consisted of a centrally located 2.94 m long section of the flume (Fig. 1a,b), screened at the upstream end by a 100 mm thick polycarbonate flow straightener (elongated tubular porosity - 7 mm diameter) to minimise incoming turbulent fluctuations, and downstream by a 10 mm diameter wire mesh, both of which prevented fish leaving. A wire mesh release chamber (0.7 m long, 0.4 m wide, and 0.5 m deep) in which the subject fish were held immediately prior to the start of each trial was connected to the experimental area by a centrally located rectangular orifice (0.2 m wide and 0.15 m high) in the downstream screen (Fig. 1a,b). Polyurethane sheeting was used to prevent light entering the experimental area and thus eliminated visual cues. Light intensities were below the threshold at which a human observer could see. Fish behaviour was recorded using low light cameras under infrared illumination.

An array of 15 vertically oriented cylinders (10 - 90 mm diameter) positioned across the flume 0.94 m downstream from the flow straightener (Fig. 1) created a complex hydrodynamic flow field with distinct regions of differing turbulent intensities and length scales. Hydrodynamic variation was greater in the x-y than in the x-z plane (i.e. lateral velocity standard deviation was consistently higher than vertical velocity standard deviation: $\sigma_v > \sigma_z$). The cylinders were spaced at a sufficient distance apart to avoid wake-interference in the near-wake region (*see:* Zhang and Zhou, 2001; Akilli *et al.,* 2004; Gao *et al.,* 2010) and to minimise areas of laminar gap-flow. This was achieved by ensuring that the axis-to-axis (or axis-to-channel boundary for the cylinder immediately adjacent to the flume wall) cylinder spacing (g_c mm) was set at a constant ratio to cylinder diameter (d mm) (Eqn 1).

$$g_c \Big/ \left(\frac{d_1+d_2}{2}\right) = 2.375 \qquad (1)$$

Fish experienced flow fields created by one of two treatments (A or B) or a control (no cylinders present) during the study (Fig. 1c). In treatment A, cylinder diameters increased incrementally across the flume width so that the smallest and largest cylinders were located adjacent to the channel lateral walls (Fig. 1c). In treatment B the combination of cylinders was switched so that the largest

Journal of Experimental Biology • Advance article

and smallest occupied locations close to the channel centre (Fig. 1c). The orientation of the cylinder array in each treatment was randomised (by rotating the array 180° about the central vertical axis) among trials to control for any hydrodynamic conditions associated with the flume. Data collected under the randomised cylinder array orientations were aggregated for each treatment. Discharge remained constant (0.15 $m^3 s^{-1}$) during each trial independent of treatment. Water depth was roughly uniform (270 mm) throughout the experimental area under the control. Under both treatments depth was greater upstream (275 mm) than downstream (265 mm) of the array due to head losses generated by the cylinders.

Instantaneous velocity in the longitudinal (*u*), transverse (*v*) and vertical direction (*w*) (Fig. 1) were measured (*n* = 671, 678 and 84 for treatments A, B, and control, respectively) using an acoustic Doppler velocimeter (ADV) (Vectrino, Nortek-AS, Norway - frequency 50 Hz, sampling volume 0.05 cm^3, record duration 3 min, distance from bed 90 mm). Raw data was filtered using a 3D velocity cross-correlation algorithm (Cea *et al.,* 2007) and the time-averaged (overbar) and fluctuating parts (prime) (e.g. $u' = u - \bar{u}$) of each instantaneous velocity component calculated, along with *U, TI,* TI_R, *TKE* and τ_{uv} (see Table 1).

Table 1. Metrics used to describe hydrodynamic conditions that fish experienced in the experimental area.

Metric	Notation	Equation	Units
Reynolds Number	R_e	$U_f d/v$	N/A (dimensionless)
Vortex shedding frequency[a]	f	StU_r/d	Hz
Wake wavelength	λ	U_f/f	mm
Estimated velocity of the restricted flow past each cylinder	U_r	$U_f\left(W/(W-\sum d)\right)$	m s^{-1}
Mean velocity	U	$(\bar{u}^2+\bar{v}^2+\bar{w}^2)^{0.5}$	m s^{-1}
Turbulence intensity	TI	$({\sigma_u}^2+{\sigma_v}^2+{\sigma_w}^2)^{0.5}$	m s^{-1}
Relative turbulence intensity	TI_R	TI/U	N/A (dimensionless)
Turbulent kinetic energy	TKE	$0.5\rho\left(\overline{u'^2}+\overline{v'^2}+\overline{w'^2}\right)$	J m^{-3}
Horizontal Reynolds shear stress	τ_{uv}	$-\rho\overline{u'v'}$	N m^{-2}
Drag	*D*	$D \propto U\sqrt{U^2+{\sigma_v}^2+{\sigma_z}^2}$	N/A (dimensionless)
Autocorrelation function of the lateral velocity component[b]	/	$\overline{v'(t)v'(t-\tau)}/\overline{v'^2}$	N/A (dimensionless)
Cross-correlation function of the lateral velocity component[b]	/	$\overline{{v_1}'(t){v_2}'(t-\tau)}/\overline{{v_1}'{v_2}'}$	N/A (dimensionless)

a: Using St = 0.2 (appropriate for the range of Reynolds numbers in this experiment [See Table S1] - Sumer and Fredsøe, 1997).
b: Using τ = 1/50 s.

Based on the Reynolds numbers (Table S1), each cylinder wake was expected to be completely turbulent with both sides of the cylinder experiencing boundary layer separation (subcritical wake regime - Sumer and Fredsøe, 1997).

Taylors Hypothesis of frozen turbulence (Taylor, 1938) (i.e. the hypothesis that turbulent-eddies are advected at or near mean flow velocity) is notoriously violated (see Pope, 2000) in the near-wake region of bluff bodies. As such, two-point simultaneous ADV measurements were used to accurately assess the convection speed of the dominant energy containing eddies (E_s) and infer TLSs. Two to five simultaneous measurements (n = 28, sample length 5 mins) were taken downstream of the central axis of each cylinder in treatment A using two longitudinally aligned (spacing 180mm) and synchronised ADVs (first ADV located 270 – 1590 mm downstream of each cylinder array). E_s was calculated as the ratio between the distance between ADVs and the time lag (τ) corresponding to the first peak appearing in the cross-correlation function of the synchronised lateral velocity data (Table 1). Well defined cross-correlation peaks were observed for the majority of simultaneous measurements, except downstream of the smallest cylinders (10 mm diameter) where eddy coherence was lost. E_s was found to be linearly related (r^2 = 0.687) and similar to the mean velocity U between the two probes ($E_s = 0.77U + 0.12$) (i.e. convection velocity was similar to flow velocity behind all cylinders). As such, it was deemed valid to use cross-section mean velocity (U_f) as a proxy for convection velocity in all treatments to calculate *TLSs* from the single point measurements as $E_d = U_f E_t/2$, where E_d is the characteristic size (m) and E_t is the turnover time (s) of the dominant energy containing eddies. E_t was calculated as the time between first and second positive peak in the autocorrelation function of the lateral velocity component (Table 1). E_d downstream of each cylinder (11 – 123 mm for the 10 - 90 mm diameter cylinders, respectively) was similar (linear trend: y=0.98x + 0) and highly correlated (r^2 = 0.975) to the estimated values (λ/2 in Table S1).

The drag force (D) acting on a fish holding its position is normally calculated as $D = 0.5\rho S U^2 C_d$ (kg m s^{-2}), where ρ is fluid density (kg m^{-3}), S is the frontal area of the fish (i.e. its maximum projection on to a plane normal to the direction of flow) (m^2), U is the mean longitudinal flow velocity (m s^{-1}), and C_d is the dimensionless drag coefficient (Webb, 1975). As sources of thrust and drag are not separable in axial undulating self-propulsion, the empirical calculation of C_d for a swimming fish is difficult (Schultz and Webb, 2002). To simplify matters, at first approximation S and C_d can be assumed to be constant (Vogel, 1996), hence $D \propto U^2$. However, this definition applies strictly only to steady flows, which are rare in natural lotic habitats. It is generally accepted that, turbulence contributes to destabilise fish and hence to increase energetic costs of swimming. This is generally

true unless turbulence displays a high level of coherence and eddies can be exploited using specialised swimming kinematics (e.g. Kármán gait, Liao *et al.,* 2003a). Turbulence can affect swimming performance in many ways. In particular, abrupt lateral and vertical velocity fluctuations prevent fish from aligning with the instantaneous flow direction and hence to fully exploit its streamlined shape to reduce form drag. This means that, instantaneously, the frontal area exposed to the incoming flow increases and drag with it. Furthermore, even in the unlikely event a fish is able to align instantaneously with the flow, vertical and lateral turbulent fluctuations will increase drag forces, because of the non-linear dependence of D on velocity. This can be easily explained by the following example: Assuming, for simplicity, a fish behaves like a sphere whose drag is insensitive to flow direction. If it holds position against a steady flow with velocity U, then the drag force it is subjected to can be computed as $D \propto U^2$. If a lateral velocity component which fluctuates between $\pm v$ is added, this has the effect of instantaneously changing the flow direction and magnitude, while keeping average lift forces (i.e. forces perpendicular to the mean flow direction) to zero (see Fig. 2). The drag force that the fluid exerts on the sphere-fish can now be computed as $D \propto (U^2 + v^2)\cos\theta$, where $\cos\theta = U/\sqrt{U^2 + v^2}$ and hence $D \propto U\sqrt{U^2 + v^2}$, which is greater than $D \propto U^2$. It is difficult to quantify the effects of turbulence to accurately compute drag forces (and hence energetic costs of swimming) acting on real fish as a response to the mechanisms described above. However, we propose that the metric outlined in Equation 2 (which also includes the influence of a vertical velocity component) does take into account such effects and represents a good proxy to quantify energetic costs of swimming in destabilising turbulent flows.

$$D \propto U\sqrt{U^2 + {\sigma_v}^2 + {\sigma_z}^2} \qquad (2)$$

Standard deviations of the lateral and vertical velocity components (σ_v and σ_z, respectively) are used as these better describe the time varying impact of these components. Although this approximation of drag is new to the field of Ecohydraulics similar approximations are used elsewhere (e.g. canopy drag - Dupont *et al.,* 2008; sedimentology - Nalpanis *et al.,* 1993). We acknowledge that this approximation of drag is static and limited to instances where fish are station holding (i.e. thrust = drag), with fish actively moving upstream likely to experience higher levels of relative drag than predicted by this metric. However, the metric represents a good proxy for assessing the likely energetic costs of holding station at different locations and hence is useful when investigating space use in relation to energy conservation strategies.

All the computed hydraulic metrics (U, TI, TI_R, TKE, τ_{uv}, E_d and D) were interpolated (Delaunay triangulation with linear interpolation) at 1mm resolution to create hydrodynamic maps of the experimental area (Fig. 3 for treatment A). As ADV measurements were not possible within 30 mm of the flume walls a fitted logarithmic function, based on measurements taken at the walls under the control, was used to estimate boundary conditions. Sensitivity analysis revealed that boundary layer estimation method (several were trialled) had little effect on overall trends. The fitted logarithmic function was used as it was thought to better represent actual conditions.

2.2. Experimental procedure

Three size classes (age cohorts) of hatchery raised brown trout were obtained so that the influence on space use of fish length and related swimming capability could be assessed. Medium and large fish were obtained from Allenbrook Trout Farm (Wimbourne, 50° 53’ 43.9” N, 1° 58’ 27.4” W) and small fish from Bibury Trout Farm (Bibury, 51° 45’ 37.5” N, 1° 50’ 08.9” W) on 15 March 2011 and 12 March 2012, respectively (Table 2). Wild trout, caught by electric fishing at Tadnoll brook, a tributary of the River Frome (Dorset, 50° 41’ 02.5” N, 2° 17’ 28.4” W) on 14 March 2012 (Table 2), were used to validate the results obtained from the more readily available hatchery fish. The Wild trout group was not divided into size classes due to the low number and small size range caught. Instead comparisons were made against an equivalent size range of hatchery fish where possible. Trout were transported to the ICER facility in aerated water and held in filtered 3000 litre holding tanks (pH: 7.5-7.8, Ammonia: 0, Nitrite: 0, Nitrate: <40, 50% weekly water change) at ambient temperature (2011: μ = 14.07˚C, σ = 3.63˚C; 2012: μ = 10.23˚C, σ = 0.80˚C). Fish were fed once daily with commercial trout pellets.

A total of 118 one-hour trials were conducted; 51 between 29 March and 7 April 2011 (medium and large hatchery trout; flume temp: $\mu = 14.80^{\circ}C$, $\sigma = 3.02^{\circ}C$), and 67 between 21 and 30 March 2012 (small hatchery and wild trout; flume temp: $\mu = 10.37^{\circ}C$, $\sigma = 0.79^{\circ}C$) (Table 2). Individual trout were allowed to acclimatise for a minimum of 1 hour in a porous container positioned within the flume before being placed into the release chamber from which they could volitionally enter the experimental area. A trial commenced once a trout entered the experimental area; fish that failed to enter within 20 minutes, or did so but became impinged on the downstream screen for more than 10 seconds, were removed and the trial terminated. Each trial lasted a maximum of 1 hour during which each trout was allowed to freely explore and utilise the experimental area. All trials were conducted between 08:00 and 18:00 (BST). Trout were used once only and were weighed (g) and measured (Fork Length [FL] – mm) at the end of each trial. The research was reviewed and sanctioned by the University of Southampton Ethical Review Board.

Table 2. Group statistics for brown trout, *Salmo trutta*, used during experiments conducted to assess hydrodynamic space use in a recirculating flume at the ICER facility (University of Southampton).

Source	*Size class*	*FL μ ± σ (Range) (mm)*	*Mass μ ± σ (Range) (g)*	*n*	*DNLRC (%)*	*Mean duration of trial (MM:SS) (μ ± σ)*	*Total duration of data available (Hr:Min:Sec)*	*Treatment Statistics*		
								Treatment	*n*	*Total duration of data available (Hr:Min:Sec)*
Hatchery	*Small*	*144.5 ± 12.5, (110-174)*	*46.8 ± 10.7, (19-70)*	*53*	*43.4*	*21:07 ± 16:31*	*10:33:26*	*Control*	*12*	*02:36:18*
								A	*19*	*04:24:08*
								B	*22*	*03:33:00*
Hatchery	*Medium*	*224.0 ± 10.0 (202-245)*	*163.5 ± 25.7, (120-200)*	*25*	*32.0*	*57:58 ± 16:04*	*16:25:26*	*Control*	*3*	*03:00:00*
								A	*14*	*10:06:59*
								B	*8*	*03:18:27*
Hatchery	*Large*	*280.7 ± 10.24 (259-294)*	*355.3 ± 31.4, (266-396)*	*26*	*3.8*	*49:46 ± 18:30*	*20:44:20*	*Control*	*4*	*03:04:04*
								A	*15*	*10:40:16*
								B	*7*	*07:00:00*
Wild	*All*	*195.2 ± 36.1 (138-247)*	*110.5 ± 54.1, (36-202)*	*14*	*21.4*	*51:49 ± 14:14*	*09:29:59*	*Control*	*5*	*01:57:21*
								A	*4*	*03:00:00*
								B	*5*	*04:32:38*

FL: Fork Length
n: Number of fish
DNLRC: Proportion of fish that did not leave the release chamber.

2.3. Fish behaviour

For each trial, fish snout positions (x and y spatial coordinates) were obtained every second from the overhead video footage (maximum of 3600 data points per trial) using Logger Pro v3.8.2 (Vernier, US) and plots of space use and space sampled created. Space sampled was deemed to be that which fell within a fish's mechanosensory field of detection (MFoD) during a trial. The threshold distance for fish to detect hydrodynamic signals using the lateral line (primary mechanosensory organ), varies depending on a number of factors (e.g. signal type, orientation, and magnitude) but is approximately 1.5 FLs (Coombs, 1999), with signal discriminability being considerable higher at closer distances. In this study, a conservative estimate of the spatial extents of a fish's MFoD, deemed to be an area within which it can fully interpret the surrounding flow field, was set as a rectangle extending 0.5FL upstream, 1.5FL downstream and 0.5FL either side of the fish snout position (Fig. S1). Computationally, the space sampled was considered to be all the discrete interpolated hydrodynamic data points (1mm resolution) that fell with a fish's MFoD during a trial (calculated at 10Hz after linear interpolation of fish snout position). Sensitivity analysis revealed that the results were relatively unsensitised to the specific size of the assigned MFoD, with a modified MFoD of half and double the size of that outlined above having little effect on overall trends.

Specialised Behavioural Zones (SBZs) expected to provide opportunities for fish to reduce the energetic costs of station holding through the expression of unique swimming kinematics (e.g. Kármán gaiting, entraining, bow riding) were identified based on information obtained from the literature (e.g. Liao *et al.* 2003a; b; Liao, 2006; Przybilla *et al.,* 2010), observation of trout during the trials, and clustering evident in the plots of space use. Using data aggregated from both treatments the proportion of time individual trout spent in each SBZ was calculated and comparisons made between: 1) observed and expected if fish had been evenly distributed throughout the experimental area (all trout: Wilcoxon signed-rank tests), and 2) wild and hatchery trout, using a sample (n = 30) of hatchery fish of equivalent size to those obtained from the wild (Mann-Whitney tests). In addition, the relationship between FL and 3) the proportion of time spent in each SBZ (all trout) and 4) the diameter of the cylinder associated with the SBZ that fish spent the highest proportion of time were assessed (Pearson's correlation with bootstrapped [n = 2000] and bias corrected confidence intervals [BCa CI]- Efron and Tibshirani, 1993).

To quantify hydrodynamic space use, preference curves were constructed for each measured metric. Hydrodynamic preference (H_p) for individual trout was calculated as $H_p = S_u/S_s$, where S_u and S_s

are histograms of space used and space sampled, respectively. The histograms were constructed by calculating the normalised frequency of space used or space sampled within the experimental area for increments (50 equally distributed bins) of each metric (for graphical representation of process see Fig. S2). S_u and S_s distributions were extrapolated from the interpolated hydrodynamic data using the discrete values (1mm resolution) that corresponded to fish snout position or that fell within a fish's MFoD, respectively, during each trial (Fig. S2). The frequency distributions were normalised to control for the elevated number of discrete data points '*sampled*' versus '*used*' during each trial. Average hydrodynamic preferences for each trout group (wild and small, medium and large hatchery trout - GH_p) were calculated for each metric as a weighted average of H_p normalised by trial duration (*TD*) (Eqn 2).

$$GH_p = \frac{\sum_{i=1}^{n} H_{pi} TD_i}{\sum_{i=1}^{n} TD_i} \qquad (2)$$

where n is the total number of trout in each group. Trends in the GH_p curves were compared to frequency distributions of total available hydrodynamic space (H_t). Trout preference for hydrodynamic space that was rarely available (< 0.1% of total area) was disregarded by assessing GH_p curves only over the range of conditions where $H_t > 0.001$. To assess the influence of specialised behaviours, GH_p curves were calculated using both unmodified and modified S_u data. The modified S_u data was constructed by identifying SBZs trout used more frequently than expected if their distribution had been even, and randomly removing the excess proportion of points that occurred within them (for graphical representation of process see Fig. S3). As such, the potential influence of specialised behaviours was removed from the modified preference curves. Differences in trends evident in the GH_p curves constructed using the modified and unmodified S_u data were visually assessed. Final conclusions in relation to hydrodynamic space use by brown trout were drawn from the GH_p curves constructed using the modified S_u data. It is acknowledged that even when confounding variables are absent space use data may be noisy due to erratic behaviour but over a large number of experimental trials it is assumed that underlying patterns evident in the group preference curves will be as a result of hydrodynamic conditions. Data analysis and visualisation was undertaken using Matlab v7.10.0.499 (MathWorks, US), SPSS v20.0.0 (IBM, US), and, SigmaPlot v12.5.038 (Systat Software Inc., US).

3. Results

Space use varied dramatically among individuals and treatments with trout tending to be thigmotactic under the control and influenced by the cylinders under the treatments (Fig. 4). Only 17.6% of trout sampled 100% of the experimental area (Mdn: 86.5%, Range: 7.0 – 100%). The extent of the experimental area sampled was not limited to the downstream section and did not follow a regular pattern (example: Fig. 4B).

The following SBZs were identified: a) *Kármán gaiting zones* - the area behind a bluff body where fish can alter their body kinematics to synchronise with the vortices shed to reduce energetic expenditure (e.g. Kármán gait) (2.5*d* to 7.5*d* downstream of each cylinder, 1*d* wide); b) *entraining zones* - the area in close proximity to the side of a bluff body where fish can hold position by tilting their body off parallel to the bulk flow to use the resulting lift and wake suction forces to mitigate for drag (e.g. Przybilla *et al.,* 2010) (-*d*/4 to 1.5*d* downstream of each cylinder, 2.375*d* wide); c) *bow riding zones* - the low-velocity high-pressure area in front of a bluff body where fish can hold position with a reduced trailing edge pressure deficit (e.g. Liao *et al.,* 2003a) (1FL to 1FL+*d* upstream of each cylinder, 1*d* wide); d) *tail holding zones* - where fish were able to hold position facing the flow by placing their tail against the downstream screen and their body along the channel wall (previously undescribed behaviour) (0.6FL to 1.2FL upstream of the downstream screen, flush with the flume wall, 0.25FL wide); and e) *wall holding zones* - the area where fish were able to hold position close to the flume wall and slightly downstream of the cylinder array with observed reduced body undulation (previously undescribed behaviour) (inline to 2.5*d* downstream of each cylinder, flush with flume wall, 2.375*d*/4 wide) (Fig. 5). Presumably the wall holding behaviour utilised spatially stable hydraulic conditions created between the cylinder and channel side, enabling fish to hold position with reduced drag. Although wall holding likely involved similar mechanisms to entraining (see Liao, 2006 and Przybilla *et al.,* 2010), it was considered a separate behaviour because kinematics and focal position were clearly influenced by the proximity of the channel sides (Fig. 5B).

The period of time spent occupying SBZs varied greatly among individuals and groups (Fig. 6). Tail holding, entraining and wall holding zones were occupied by individual trout for a much higher proportion of a trial than expected (up to 86, 64 and 33 %, respectively) if space use had been even throughout the experimental area (Fig. 6). At a group level tail holding regions, by small (z = 4.107, p < 0.001), medium (z = 2.896, p < 0.01), and large (z = 3.173, p < 0.001) hatchery trout, and wall holding regions, by large hatchery trout (z = 3.363, p < 0.001), were consistently used more frequently than expected if distribution had been even (Fig. 6). There was no difference in the

percentage of time wild trout spent in each zone compared to hatchery trout of equivalent size. Smaller hatchery fish spent a higher proportion of time in tail holding (r_s = -0.428, p < 0.001, 95% BCa CI: -0.571, -0.250) and a lower proportion in the Kármán gaiting (r_s = 0.5451, p < 0.001, 95% BCa CI: 0.301, 0.588) and bow riding (r_s = 0.242, p < 0.05, 95% BCa CI: 0.072, 0.462) zones than larger trout (Fig. S4). There was no correlation between FL and the proportion of time spent in the entraining or wall holding zones. Smaller trout were more likely to use entraining zones associated with smaller cylinders than larger trout (r_s = 0.599, p<0.01, 95% BCa CI: 0.244, 0.835) (Fig. S5). There was no correlation between FL and cylinder diameter in relation to the Kármán gaiting or bow riding zones which trout used.

The key difference resulting from the two ways of calculating GH_p (with modified vs. unmodified S_u data) was the absence of an additional peak in the U and D preference curves constructed using the modified S_u data (for example see Fig. 7). The additional peaks in the GH_p curves constructed using the unmodified S_u data represent the influence of fish occupying space where specialised behaviours could be exhibited.

GH_p curves constructed using modified S_u data for trout group, treatment, and hydrodynamic metric are presented in Figure 8. Preference for specific areas was highest (up to 25 times) for *U* and *D*, with the majority of groups preferentially using areas with lower *U* and *D* than was most frequently available under each treatment and the control (exception: large fish in Treatment B). Preference for low drag areas was generally higher for wild and small hatchery trout than medium or large fish. In treatment A and B, preference for *TI*, TI_R, *TKE*, and τ_{uv} followed the H_t histograms, being higher for areas with low levels of each metric. There were a few exceptions, which included a slight preference exhibited by large fish for areas of high *TKE* (12.3 J m^{-2}: 1.1 times) and τ_{uv} (7.8 N m^{-3}: 1.8 times) in treatment A and B, respectively. Under the control all groups preferentially used areas with higher than most frequently available *TI*, TI_R, *TKE*, and τ_{uv}. However, the range and magnitude of turbulence available was low. Trout preference for E_d differed for each group under each treatment. Under treatment A, peak preference of wild and small, medium and large hatchery trout was for areas where E_d = *ca.* 0, 10, 40, and 60mm, respectively. Medium and large hatchery trout also exhibited an additional slight preference (*ca.* 1.3 times) for areas where E_d = *ca.* 125-140 mm. Under treatment B, peak preference of small hatchery trout was for areas with very small E_d (*ca.* 5 mm) but wild and medium and large hatchery trout showed no clear preference for E_d of any size.

4. Discussion

Although it is widely accepted that animal distributions reflect a trade-off between the energetic benefits and costs of the microhabitat selected, for stream dwelling fish the identification of the most appropriate hydrodynamic predictors of space use is the focus of much debate (Lacey *et al.* 2012). In previous studies a variety of metrics and approaches have been adopted, ranging from simplistic empirical measures of unidirectional velocity in the laboratory (e.g. Baldes and Vincent, 1969) or field (e.g. Conallin *et al.,* 2014) to the outputs of numerical modelling of complex flows (e.g. Crowder and Diplas, 2006). Unfortunately, the variables used tend to lack biological realism because they provide a poor indirect proxy for some more ecologically relevant factor, while the approaches employed frequently fail to account for multiple confounding variables. In this study we took a reductionist approach to define space use of brown trout under complex non-laminar flows in the laboratory in which density dependent (conspecifics) and other confounding factors (e.g. visual cues, food, predators) were absent. A simple, robust and biologically relevant descriptor of drag that incorporates both mean and fluctuating velocity components provided a realistic surrogate for the energetic cost of holding station. Maximising the ratio of energetic benefits to costs is commonly surmised as the principle driver for space use (e.g. Bachman, 1984 for brown trout) but it seems to be frequently overlooked. In this study, we demonstrated that, as hypothesised, energy conservation strategies play a key role in space use in an energetically taxing environment with the majority of trout groups choosing to frequently occupy areas where specialised behaviours could be adopted or by selecting low drag regions.

Independent consideration of drag when describing the distribution and movement of fish is not new. For example McElroy *et al.,* (2012), using a drag based energetic cost function, found that pallid sturgeon (*Scaphirhynchus albus*) select less costly migratory routes and Hughes (2004) proposed the avoidance of 'wave drag' as the cause behind discrepancies in the expected vs. observed pathways of salmonids during their spawning migration. Further, the importance of turbulence is well recognised, and a variety of different metrics (e.g., *TI*: Smith *et al.,* 2005, TI_R*:* Cotel *et al.,* 2006, *TKE*: Smith *et al.,* 2006, and τ: Hayes and Jowett, 1994; Silva *et al.* 2011; 2012a and 2012b; Duarte *et al.,* 2012) have been used to define suitable habitat or migratory routes, although such statistical links remain difficult to interpret from an ecological perspective. However, attempts to quantify hydrodynamic space use by fish living in lotic environments frequently fail to consider both drag and turbulence together. Definitions of drag previously used fail to account for turbulent fluctuations that occur under unsteady flows common in nature, and as a result likely underestimate energetic

costs. Unless specific conditions are met it is generally accepted that turbulence reduces swimming performance (e.g. Lupandin, 2005; Tritico and Cotel, 2010) and increases the cost of swimming (e.g. Enders *et al.,* 2003; 2004; 2005). Hence a combination of both mean velocity and turbulence in a drag metric provides a simple and more biologically relevant hydraulic descriptor than mean velocity and / or a separate measure of turbulence alone. In this study, peaks observed in the drag preference curves were also evident in the mean velocity (*U*) data. This was expected because under the flow configurations created *U* was generally a lot higher than its variation laterally (σ_v) or vertically (σ_z) (i.e. a lot higher than velocity variation due to turbulence). However, trends in space use were clearer in the drag than the mean velocity preference curves because the incorporation of the influence of turbulence (lateral and vertical velocity fluctuations) in the drag metric refined its predictive power. Hence, although in this study U provided a good proxy for drag and concurrently energetic expenditure, it is likely that in other situations with higher intensities of turbulence (e.g. within fish passes) this may not be the case. In any case, drag, either simply derived (e.g. $D \propto U^2$) or after incorporating turbulent fluctuations, is conceptually a more ecologically meaningful metric to describe space use than mean velocity, as it has direct implications for energetic expenditure during swimming. It is interesting to note that for the majority of fish groups, a sharp maximum in the preference curves occurred for *D* = *ca.* 0.12. It is likely that this was the lowest available level of drag that fish could effectively exploit, with even lower values occurring at locations in close proximity of solid boundaries that were inaccessible to fish due to their size.

Under certain circumstances fish can exhibit performance enhancing behaviours (e.g. Kármán gaiting: Liao *et al.,* 2003b, entraining: Przybilla *et al.,* 2010, bow riding: Taguchi and Liao, 2011) that reduce the energetic costs associated with the lotic space selected. Such behaviours are commonly observed in nature, e.g. when trout associate with zones upstream or downstream of boulders and bridge footings or other similar natural or artificial structures. In this study, areas of the experimental arena in which fish were predicted able to benefit from specialised performance enhancing behaviours were identified. In addition to those previously described, trout exhibited two additional behaviours: wall and tail holding. 'Wall holding', although similar to entraining as defined by Liao (2006) and Przybilla *et al.* (2010), was considered distinctly different because focal position was clearly influenced by the proximity of the channel side. It is likely under these conditions that the boundary layer modified local flow conditions and altered the direction of the resulting forces acting on the fish (e.g. lift and drag). Similar 'wall holding' clustering was depicted by Przybilla *et al.* (2010 - Fig. 2) but was not analysed or discussed. During 'tail holding' fish utilised a physical object to rest against (the downstream mesh screen), rather than exploiting spatial and/or temporal

variations in hydrodynamics to gain an energetic advantage. Out of all the potential specialised behaviours identified, individual fish spent the highest proportion of time in tail holding, followed by entraining, and then wall holding zones and at a group level tail holding and wall holding zones were consistently used. Individual trout utilised tail holding zones for extended periods of a trial (up to 86 %) with almost no corrective fin movement or body undulation (pers. obs.), suggesting that this is the most energetically efficient mode of station holding under the experimental setting described.

Behaviours and distribution relative to the cylinder array varied with body size. As expected (e.g. Beamish, 1978), smaller fish had a lower swimming performance than larger fish, as indicated by shorter swim periods before becoming impinged against the downstream screen. Small fish also spent a higher proportion of time occupying low drag zones and areas where they could exploit the most energy efficient tail holding strategy, whilst large hatchery fish were more likely to maintain position in wall holding zones. Indeed the only fish group not to display a peak preference for space with lower *D* than that most frequently available was the large fish in Treatment B, likely due to their reduced need to conserve energy. There was also a positive relationship between body length and the diameter of cylinders on which trout tended to entrain (Fig. S5), suggesting hydrodynamic characteristics of proportional scale to fish length are beneficial, if not required, for this behaviour. The critical size of eddies required to destabilise a fish has been found to be approximately equivalent to body length (Pavlov *et al.,* 2000; Lupandin, 2005, Tritico and Cotel, 2010). Therefore, small trout may have been destabilised by eddies produced downstream of the larger cylinders, an expectation supported by the observation under one cylinder arrangement (treatment A) in which medium and large hatchery trout tended to associate with areas with large eddy diameters, whereas smaller trout tended to associate with areas with smaller eddy size.

This study represents a step forward in understanding fish behaviour under hydrodynamically complex settings. We have shown that time-averaged single point hydraulic metrics alone cannot accurately predict space use by fish under complex flows if specialised performance enhancing behaviours that rely on spatial and temporal variation in flow are not accounted for. However, when specialised behaviours are accounted for it was shown that a novel definition of drag allows for clear predictions of space use and that it is a more ecologically relevant predictor of space use than other commonly utilised metrics. Our observations provide empirical evidence that energy conservation strategies play a key role in space use by fish. These findings and the methods outlined in this paper have important implications for fish management practices, including the development of effective habitat suitability models, river restoration, and fish passage. The results are robust as preference

for space use was quantified by taking into account the sampled rather than the available hydrodynamic environment. This represents an improvement to the standard and potentially erroneous use-vs.-availability preferences curves commonly used (e.g. Mäki-Petäys *et al*., 1997). Future research should incrementally introduce additional factors (e.g. competitors, predators, food) to advance understanding of fish behaviour under the effects and the interaction of multiple variables, which characterize more realistic conditions typical of field settings.

Acknowledgements

We thank the members of the ICER team who kindly dedicated their time to assist with trials.

Competing Interests

No competing interests declared

Author contributions

This study was planned, undertaken and analysed by Kerr, J.R.. Methodological guidance was received from both co-authors throughout the experimental period. Manes, C. helped with data analysis. All authors contributed to the writing of the manuscript.

Funding

This research formed part of PhD studentship funded by the Engineering and Physical Sciences Research Council.

5. References

Akilli, H., Akar, A. and Karakus, C. (2004). Flow characteristics of circular cylinders arranged side-by-side in shallow water. *Flow Meas. Instrum.* **15**, 187-197.

Anderson, E. J., McGillis, W. R. and Grosenbaugh, M. A. (2001)**.** The boundary layer of swimming fish. *J. Exp. Biol.* **204**, 81-102.

Bachman, R. A. (1984). Foraging behaviour of free-ranging wild and hatchery brown trout in a stream. *Trans. Am. Fish. Soc.* **113**(1), 1-32.

Baldes, R. J. and Vincent, R. E. (1969). Physical parameters of microhabitats occupied by brown trout in an experimental flume. *Trans. Am. Fish. Soc.* **98**, 230-238.

Beyer, H. L, Haydon, D. T., Morales, J. M., Frair, J. L., Hebblewhite, M., Mitchell, M. and Matthipoulos, J. (2010). The interpretation of habitat preference metrics under use–availability designs. *Philos. Trans. R. Soc. Lond. A* **365**, 2245-2254.

Bovee, K. D. (1986). Development and evaluation of habitat suitability criteria for use in the instream flow incremental methodology. Instream Flow Information Paper #21 FWS/OBS-86/7. Washington, DC: USDI Fish and Wildlife Service. pp235.

Beamish, F. W. H. (1978). Swimming capacity. In *Fish Physiology Volume 7* (ed. W. S. Hoar and D. J. Randall), pp. 101-187. New York, USA: Academic Press.

Biewener, A. A. (2003). *Animal locomotion*. New York, USA: Oxford University Press.

Cea, L., Puertas, J. and Pena, L. (2007). Velocity measurements on highly turbulent free surface flow using ADV. *Exp. Fluids*. **42**, 333-348.

Chesney, E. J. (1989). Estimating the food requirements of striped bass larvae *Morone saxatilis*: effects of light, turbidity and turbulence. *Mar. Ecol. Prog. Ser.* **53**, 191-200.

Conallin, J., Boegh, E., Olsen, M., Pedersen, S., Dunbar, M. J. and Jensen, J. K. (2014). Daytime habitat selection for juvenile parr brown trout (*Salmo trutta*) in small lowland streams. *Knowl. Manag. Aquat .Ecosyst.* **413**, 09.

Coombs, S. (1999). Signal detection theory, lateral-line excitation patterns and prey capture behaviour of mottled sculpin. *Anim. Behav*. **58**, 421-430.

Cotel, A. J., Webb, P. W. and Tritico, H. (2006). Do brown trout choose locations with reduced Turbulence? *Trans. Am. Fish. Soc.* **135**, 610-619.

Crowder, D. W. and Diplas, P. (2006). Applying spatial hydraulic principles to quantify stream habitat. *River Res. Appl.* **22**, 79–89.

Daniel, T. L. (1981). Fish mucus: *In situ* measurements of polymer drag reduction. *Biol. Bull.* **160**, 376-378.

Dean, B. and Bhushan, B. (2010). Shark-skin surfaces for fluid-drag reduction in turbulent flow: a review. . *Philos. Trans. R. Soc. Lond. A* **368**, 4775-4806.

DeGraaf, D. A. and Bain, L. H. (1986). Habitat use by and preferences of juvenile Atlantic salmon in two Newfoundland Rivers. *Trans. Am. Fish. Soc.* **115**(5), 671-681.

Duarte, B. A. F., Romos, I. C. R. and Santos, H. A. (2012). Reynolds shear-stress and velocity: Positive biological response of neotropical fishes to hydraulic parameters in a vertical slot fishway. *Neotrop. Ichthyol.* **10**(4), 813-819.

Dupont, S., Brunet, Y. and Finnigan, J. J. (2008). Large-eddy simulation of turbulent flow over a forested hill: Validation and coherent structure identification. *Q. J. R. Meteorol. Soc.* **134**, 1911-1929.

Efron, B. and Tibshirani, R. (1993). *An Introduction to the bootstrap*. *New York, USA: Chapman and Hall.*

Enders, E. C., Boisclair, D. and Roy, A. G. (2003). The effect of turbulence on the cost of swimming for juvenile Atlantic salmon. *Can. J. Fish. Aquat. Sci.* **60**, 1149-1160.

Enders, E. C., Boisclair, D. and Roy, A. G. (2004). The cost of habitat utilization of wild, farmed, and domesticated juvenile Atlantic salmon (*Salmo salar*). *Can. J. Fish. Aquat. Sci.* **61**, 2302-2313.

Enders, E. C., Boisclair, D. and Roy, A. G. (2005). A model of total swimming costs in turbulent flow for juvenile Atlantic salmon (*Salmo salar*). *Can. J. Fish. Aquat. Sci.* **62**, 1079-1089.

Enders, E. C., Roy, M. L., Ovidio, M., Hallot, E. J., Boyer, C., Petit, F. and Roy, A. G. (2009). Habitat choice by Atlantic salmon parr in relation to turbulence at a reach scale. *N. Am. J. Fish. Manage.* **30**, 1819-1830.

Facey, D. E. and Grossman, G. D. (1992). The relationship between water velocity, energetic costs, and microhabitat selection use in four North American Stream fishes. *Hydrobiologia* **239**, 1-6.

Fausch, K.D. (1984). Profitable stream positions for salmonids: relating specific growth rate to net energy gain. *Can. J. Zool.* **62**(3): 441-451.

Gao, Y., Yu, D., Tan, S., Wang, X. and Hao, Z. (2010). Experimental study on the near wake behind two side-by-side cylinders of unequal diameters. *Fluid Dyn. Res.* **42**(5), 1-13.

Hayes, J. W. and Jowett, I. G. (1994). Microhabitat models of large drift-feeding brown trout in three New Zealand rivers. *N. Am. J. Fish. Manage.* **14**, 710-725.

Heggenes, J., Northcote, T. G. and Peter, A. (1991). Seasonal habitat selection and preferences by cutthroat trout (*Oncorhynchus clarki*) in a small coastal stream. *Can. J. Fish. Aquat. Sci.* **48**(8), 1364-1370.

Hughes, N. F. (2004). The wave-drag hypothesis: an explanation for size-based lateral segregation during the upstream migration of salmonids. *Can. J. Fish. Aquat. Sci.* **61**, 103-109.

Jenkins, A. R. and Keeley, E. R. (2010). Bioenergetic assessment of habitat quality for stream-dwelling cutthroat trout (*Oncorhynchus clarkii bouvieri*) with implications for climate change and nutrient supplementation. *Can. J. Fish. Aquat. Sci.* **67**,371-385.

Jowett, I. G. and Richardson, J. (1995). Habitat preferences of common, riverine New Zealand native fishes and implications for flow management. *N. Z. J. Mar. Freshwater Res.* **29**(1), 13-23.

Krebs, J. R. (1978). Optimal foraging: Decision rules for predators . In *Behavioural Ecology: An Evolutionary Approach* (ed. J. R. Krebs and N. B. Davies), pp. 23-63. Massachusetts, USA: Sinauer Associates Inc.

Lacey, R. W. J., Neary, V. S., Liao, J. C., Enders, E. C. and Tritico, H. (2012). The IPOS framework: linking fish swimming performance in altered flows from laboratory experiments to rivers. *River Res. Appl.* **28**, 429-443.

Liao, J. C., Beal, D. N., Lauder, G. V. and Triantafyllou, M. S. (2003a). The Karman gait: novel body kinematics of rainbow trout swimming in a vortex street. *J. Exp. Biol.* **206**, 1059-1073.

Liao, J. C., Beal, D. N., Lauder, G. V. and Triantafyllou, M. S. (2003b). Fish exploiting vortices decrease muscle activity. *Science* **302**, 1566-1569.

Liao, J. C. (2004). Neuromuscular control of trout swimming in a vortex street: implications for energy economy during the Karman gait. *J. Exp. Biol.* **207**(20), 3495-3506.

Liao, J. C. (2006). The role of the lateral line and vision on body kinematics and hydrodynamic preference of rainbow trout in turbulent flow. *J. Exp. Biol.* **209**, 4077-4090.

Lupandin, A. I. (2005). Effect of flow turbulence on swimming speed of fish. *Biol. Bull.* **32**(5), 461-466.

Maertens, A.P., Triantafyllou, M.S. and Yue, D.K.P. (2015). Efficiency of fish propulsion. *Bioinspir. Biomim.* **10**, 046013.

Maynard Smith, J. (1978). Optimization theory in evolution. *Annu. Rev. Ecol. Evol. Syst.* **9**, 31-56.

Mäki-Petäys, A., Muotka, T., Huusko, A., Tikkanen, P. and Kreivi, P. (1997). Seasonal changes in habitat use and preference by juvenile brown trout, *Salmo trutta*, in a northern boreal river. *Can. J. Fish. Aquat. Sci.* **54**, 520-530.

McElroy, B., DeLonay, A. and Jacobson, R. (2012). Optimum swimming pathways of fish spawning migrations in rivers. *Ecology* **93**(1), 29-34,

Moorcroft, P. R. (2012). Mechanistic approaches to understanding and predicting mammalian space use: recent advances, future directions. *J. Mammal.* **93**(4), 903-916.

Nalpanis, P., Hunt, C. R. J. and Barret, C. F. (1993). Saltating particles over flat beds. *J. Fluid Mech*. **251**, 661-685.

Parker, G. A. and Maynard Smith, J. (1990). Optimality theory in evolutionary biology. *Nature* **438**, 27-33.

Pavlov, D. S., Lupandin, A. I. and Skorobogatov, M. A. (2000). The effects of flow turbulence on the behaviour and distribution of fish. *J. Ichthyol.* 40(2), S232-S261.

Pope, S. B. (2000). *Turbulent flows*. Cambridge, UK: Cambridge University Press.

Przybilla, A., Kunze, S., Rudert, A., Bleckmann, H. and Brücker, C. (2010). Entraining in trout: a behavioural and hydrodynamic analysis. *J. Exp. Biol.* **213**, 2987-2996.

Silva, A. T., Santos, J. M., Ferreira, M. T., Pinheiro, A. N. and Katopodis, C. (2011). Effects of water velocity and turbulence on the behaviour of Iberian barbell (*Luciobarbus bocagei*, Steindachner 1864) in an experimental pool-type fishway. *River Res. Appl.* **27**, 360-373.

Silva, A. T., Katapodis, C., Santos, J. M., Ferreira, M. T. and Pinheiro, A. N. (2012a). Cyprinid swimming behaviour in response to turbulent flow. *Ecol. Eng.* **44**, 314-328.

Silva, A. T., Santos, J. M., Ferreira, M. T., Pinheiro, A. N. and Katapodis, C. (2012b). Passage efficiency of offset and straight orifices for upstream movements of Iberian barbell in a pool-type fishway. *River Res. Appl.* **28**, 529-542.

Schultz, W. W. and Webb, P. W. (2002). Power requirements of swimming: Do new methods resolve old questions? *Integr. Comp. Biol.* **42**, 1018-1025.

Smith, D. L., Brannon, E. L. and Odeh, M. (2005). Response of juvenile rainbow trout to turbulence produced by prismatoidal shapes. *Trans. Am. Fish. Soc.* **134**, 741-753.

Smith, D. L., Brannon, E. L., Shafii, B. and Odeh, M. (2006). Use of the average and fluctuating velocity components for estimation of volitional rainbow trout density. *Trans. Am. Fish. Soc.* **135**, 431-441.

Sumer, M. and Fredsøe, J. (1997). *Hydrodynamics around cylindrical structures. Advancing Series on Ocean Engineering volume 12.* London, UK: *World Scientific Publishing Co.*

Taguchi, M. and Liao, J. C. (2011). Rainbow trout consume less oxygen in turbulence: the energetics of swimming behaviours at different speeds. *J. Exp. Biol.* **214**, 1428-1436.

Taylor, G. I. (1938). The spectrum of turbulence. *Proc. R. Soc. Lond.* **164**, 476-490.

Tritico, H. M. and Cotel, A. J. (2010). The effects of turbulent eddies on the stability and critical swimming speed of creek chub (*Semotilus atromaculatus). J. Exp. Biol.* **213**, 2284-2293.

Vogel, S. (1996). *Life in moving fluids: The physical biology of flow*. New Jersey, USA: Princeton University Press.

Webb, P. W. (1975). Hydrodynamics and energetics of fish propulsion. *Bull. Fish. Res. Board Can.* **190**, 1-159.

Webb, P. W. and Cotel, A. J. (2010). Turbulence: Does vorticity affect the structure and shape of body and fin propulsors. *Int. Comp. Biol.*, **50**, 1155-1166.

Weihs, D. (1974). Energetic advantages of burst swimming of fish. *J. Theor. Boil.* **48**, 215-229.

Zhang, H.J. and Zhou, Y. (2001). Effect of unequal cylinder spacing on vortex streets behind three side-by-side cylinders. *Phys. Fluids* **13**(12), 3675-3686.

Figures

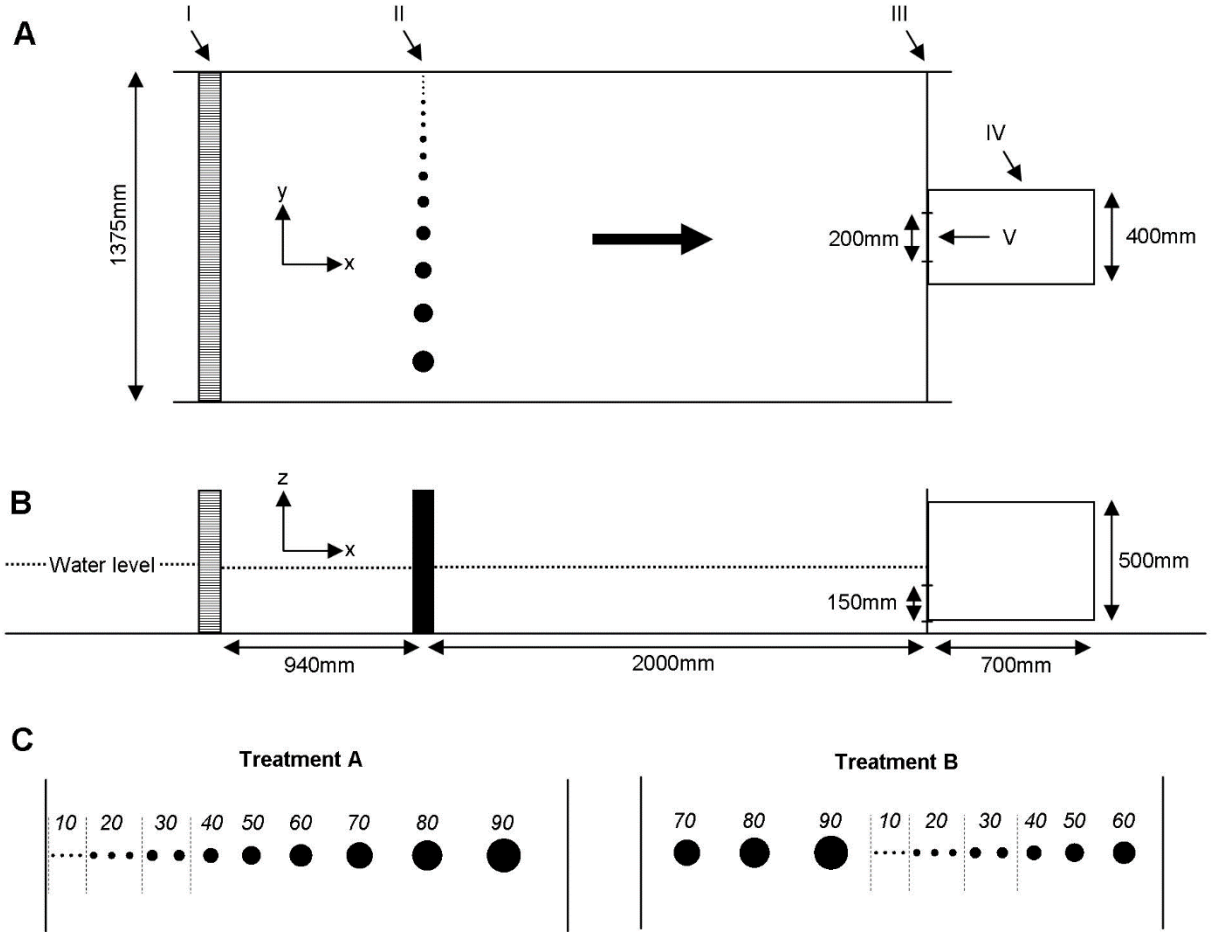

Figure 1. Plan (A) and profile (B) of the experimental area in a large recirculating flume at the ICER facility (University of Southampton) in which hydrodynamic space use of brown trout, *Salmo trutta*, was assessed. I) flow straightening device, II) cylinder array, III) mesh screen, IV) release chamber, V) release chamber orifice. Thick arrow indicates direction of bulk flow. C) The two arrangements of vertically oriented cylinders used in the treatments. Numbers indicate the diameters of the cylinders (mm). Dashed lines delineate groups of cylinders of equivalent size.

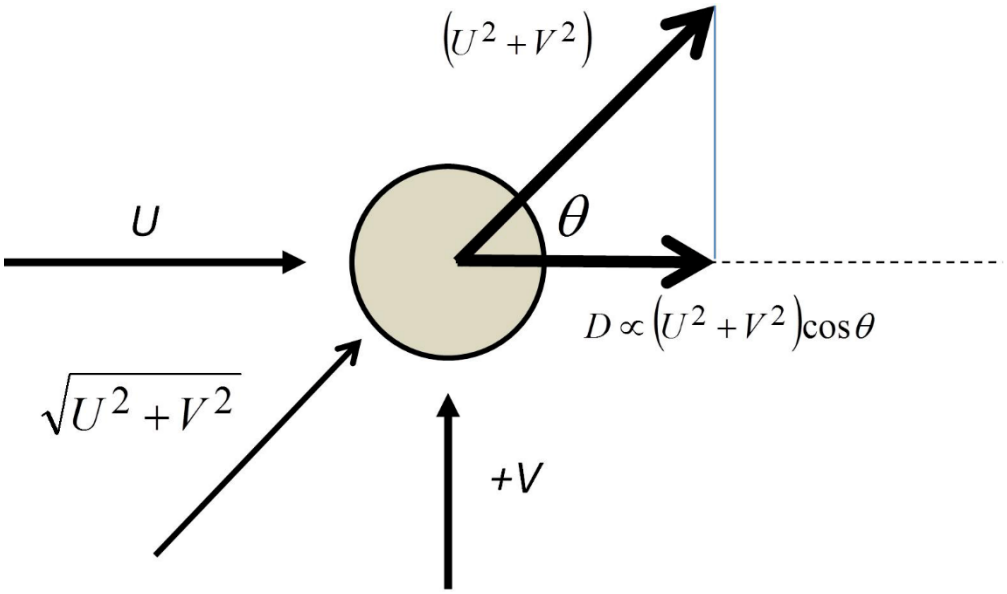

Figure 2. Diagram of the directional forces on a sphere and drag ($\boldsymbol{D}$) acting parallel to the mean flow ($\boldsymbol{U}$) as a result of an instantaneous lateral velocity component ($\boldsymbol{v}$).

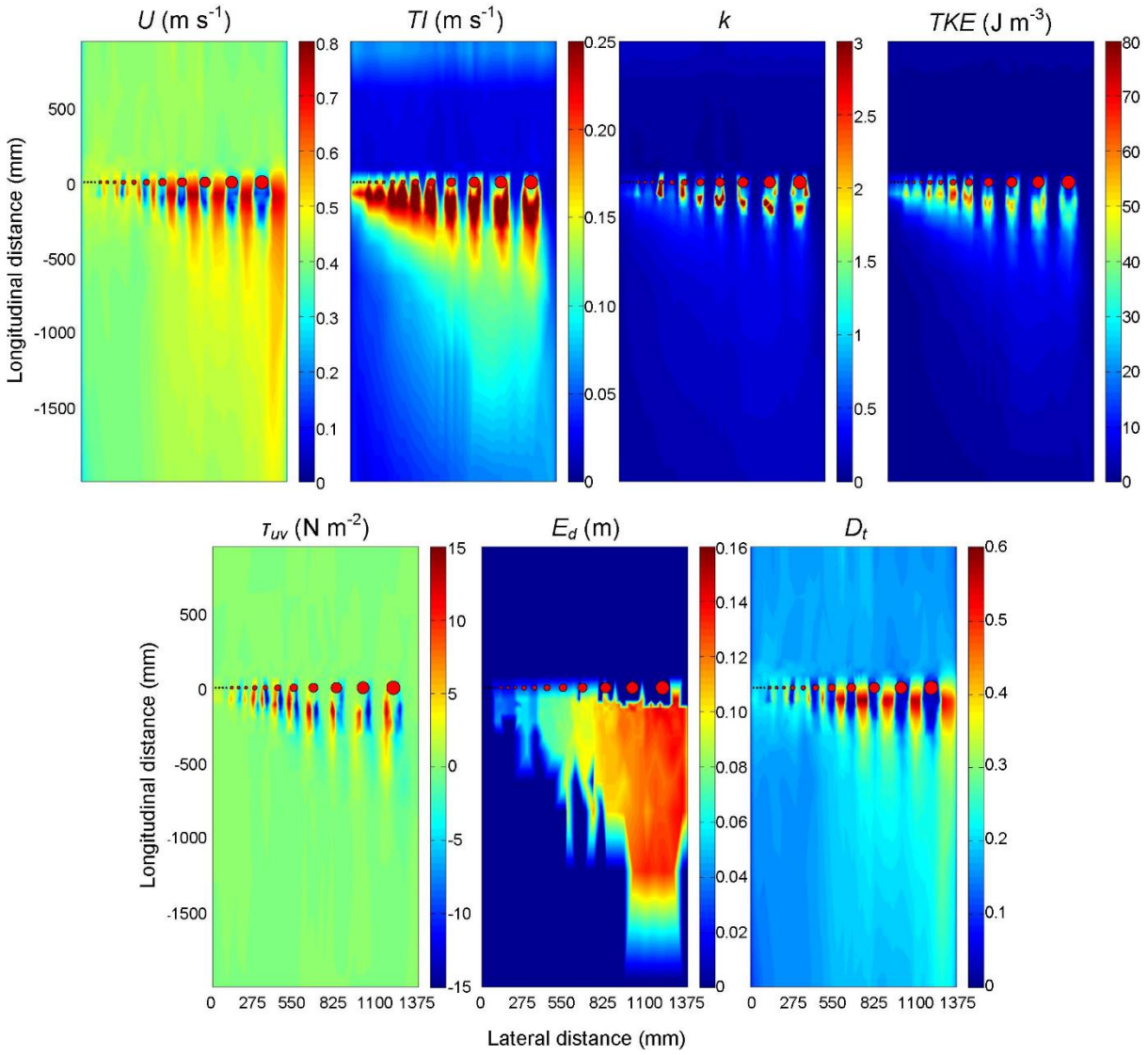

Figure 3. Colour intensity plots of mean velocity (U) (m s^{-1}), turbulence intensity (TI) (m s^{-1}), relative turbulence intensity (TI_R), turbulent kinetic energy (TKE) (J m^{-3}), horizontal Reynolds shear stress (τ_{uv}) (N m^{-2}), eddy diameter (E_d) (m) and drag (D) for treatment A in which the behaviour of brown trout, *Salmo trutta*, was assessed.

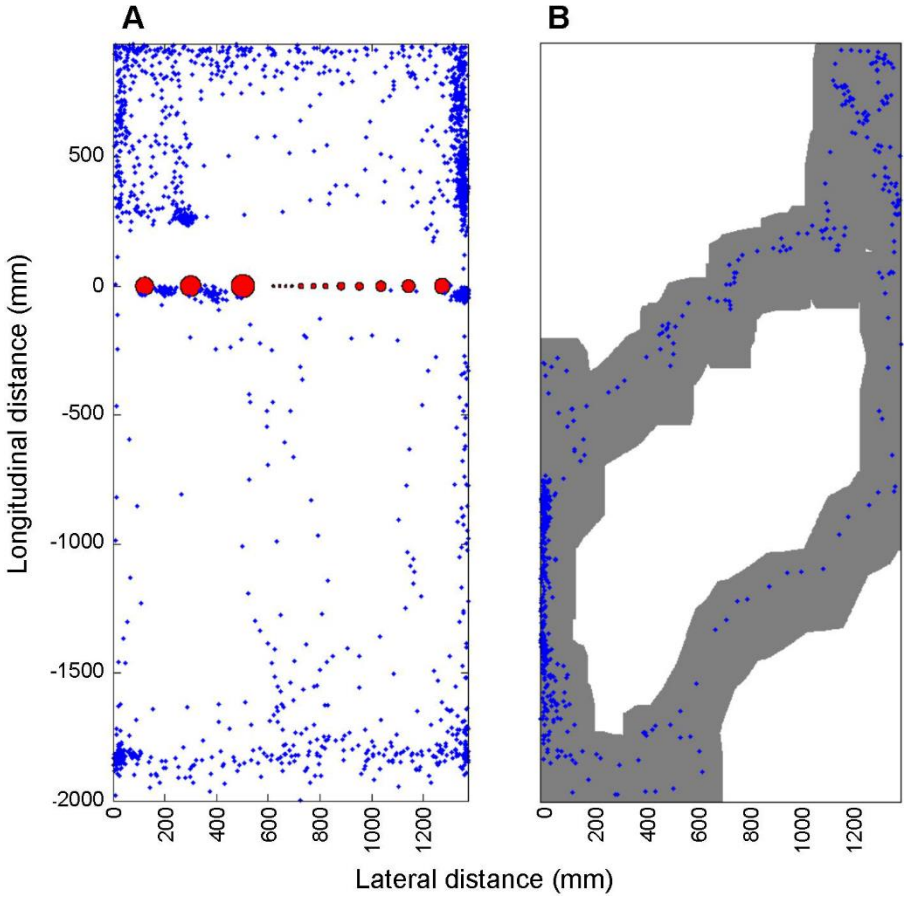

Figure 4. Example of: A) space use (S_u) by a wild trout (FL: 223mm) under treatment B (Trial 72, duration: 3507 seconds), and B) space sampled (H_s) (grey area) by a small hatchery fish (FL: 154mm) under the control (Trial 120, duration: 856 seconds). Blue dots represent snout positions of the fish tracked at 1 second intervals during the trial. The grey area corresponds to the area that fell within the fishes Mechanosensory Field of Detection (MFoD) as the fish moved through the experimental area. Mean flow direction is from top to bottom.

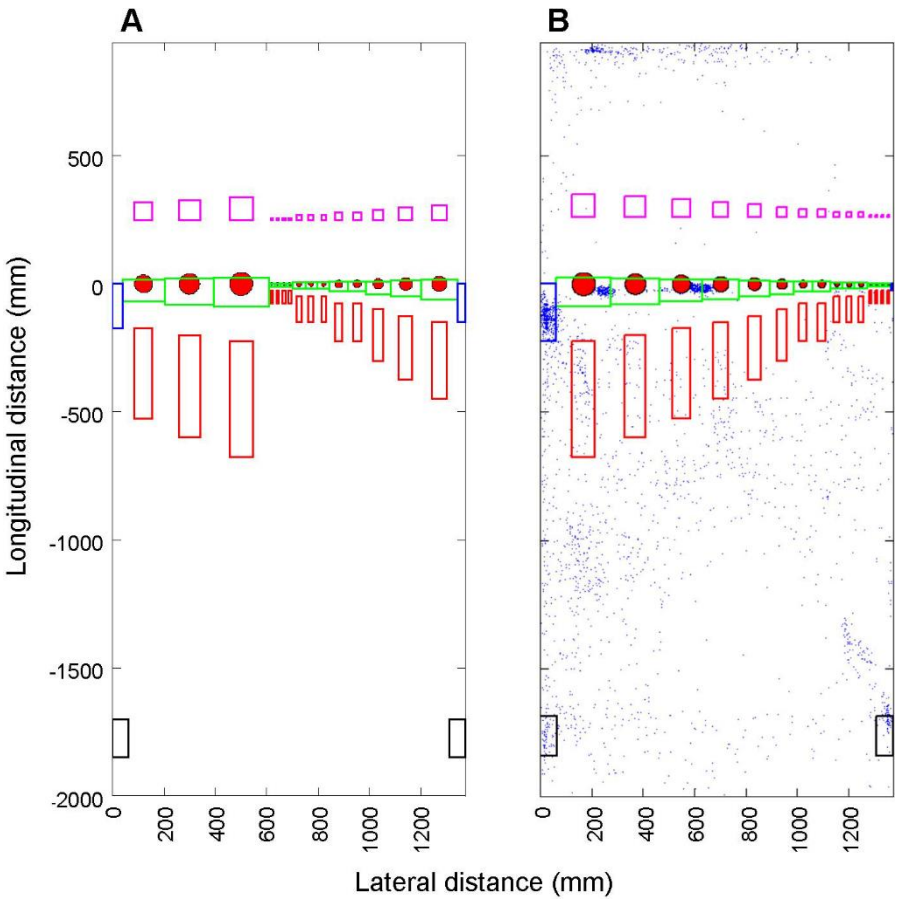

Figure 5. A) Predicted SBZs: Kármán gaiting zones (red), entraining zones (green), bow riding zones (magenta), wall holding zones (blue) and tail holding zones (black) for a 285 mm long (FL) trout under treatment B; and B) space use (blue dots represent snout positions – 1Hz) by a hatchery trout (FL: 260 mm) under treatment A (Trial 13, duration: 3356 seconds) with SBZs overlaid to emphasize the heavy use of entraining and wall holding zones and moderate use of tail holding and Kármán gaiting zones.

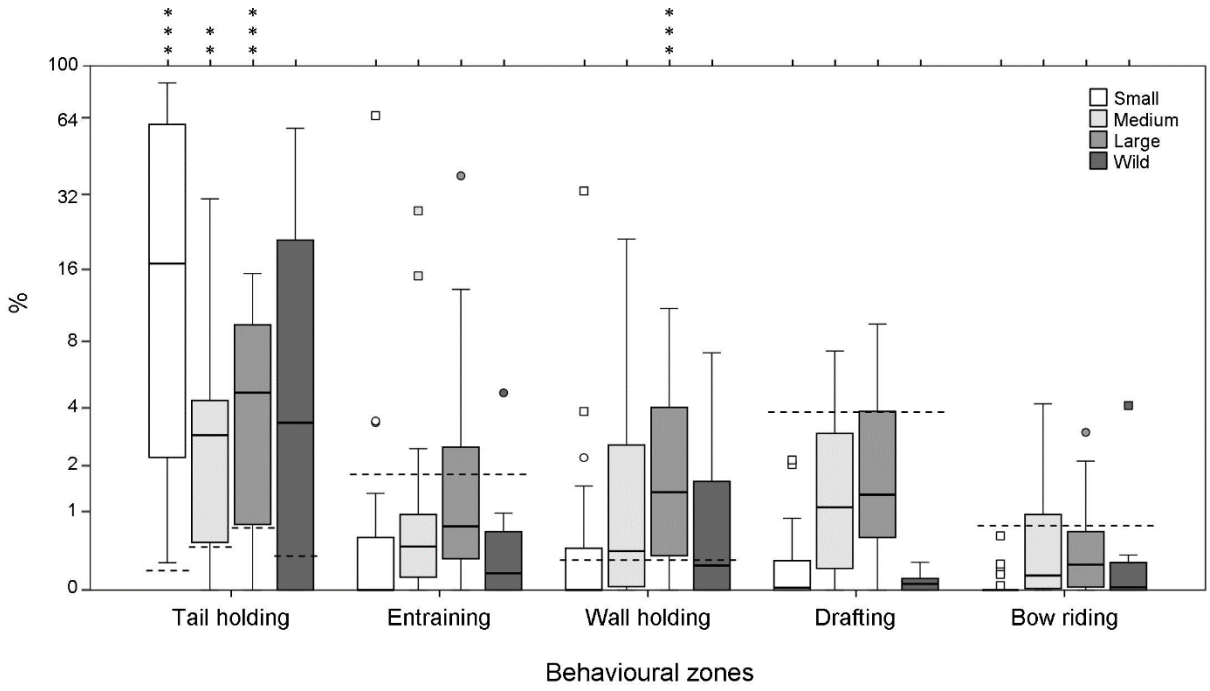

Figure 6. Box plot of percentage of the trial that wild and small, medium, and large hatchery brown trout, *Salmo trutta*, spent within the tail holding, entraining, wall holding, Kármán gaiting and bow riding zones (data pooled from treatment A and B). Boxes represent interquartile range (IQR) and median. Whiskers represent the total range excluding standard (circles) and extreme (squares) outliers (greater than the upper quartile + 1.5 or 3 times the IQR, respectively). Dashed lines represent the proportion expected if distribution had been even. Asterisks represent incidences where the proportion of time spent within a region by individuals was consistently greater than that expected if distribution had been even (Wilcoxon signed-rank tests, * = $p<0.05$, ** = $p<0.01$, *** = $p<0.001$). Note: Logarithmic scale for easier interpretation.

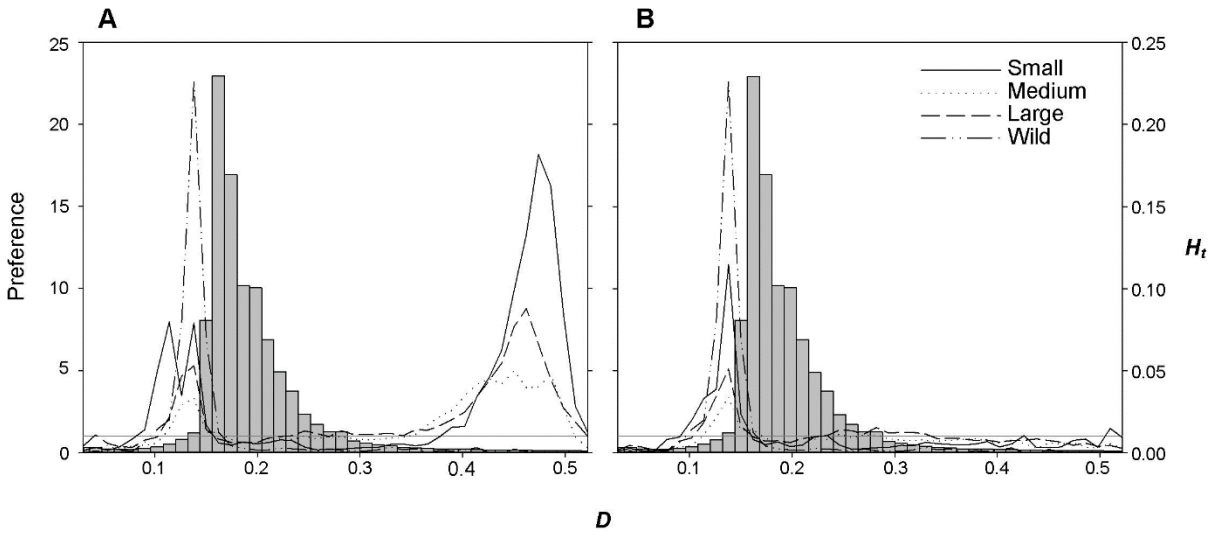

Figure 7. Drag (*D*) group hydrodynamic preference (GH_p) curves constructed using unmodified (A) and modified (B) space use (S_u) data for all wild and small, medium and large hatchery brown trout, *Salmo trutta*, in treatment A (n = 30). Left axis is group preference curve series scale and right axis is total available hydrodynamic space histogram (H_t) scale (grey bars). Solid grey line is for reference purposes and represents an even distribution (i.e. preference=1).

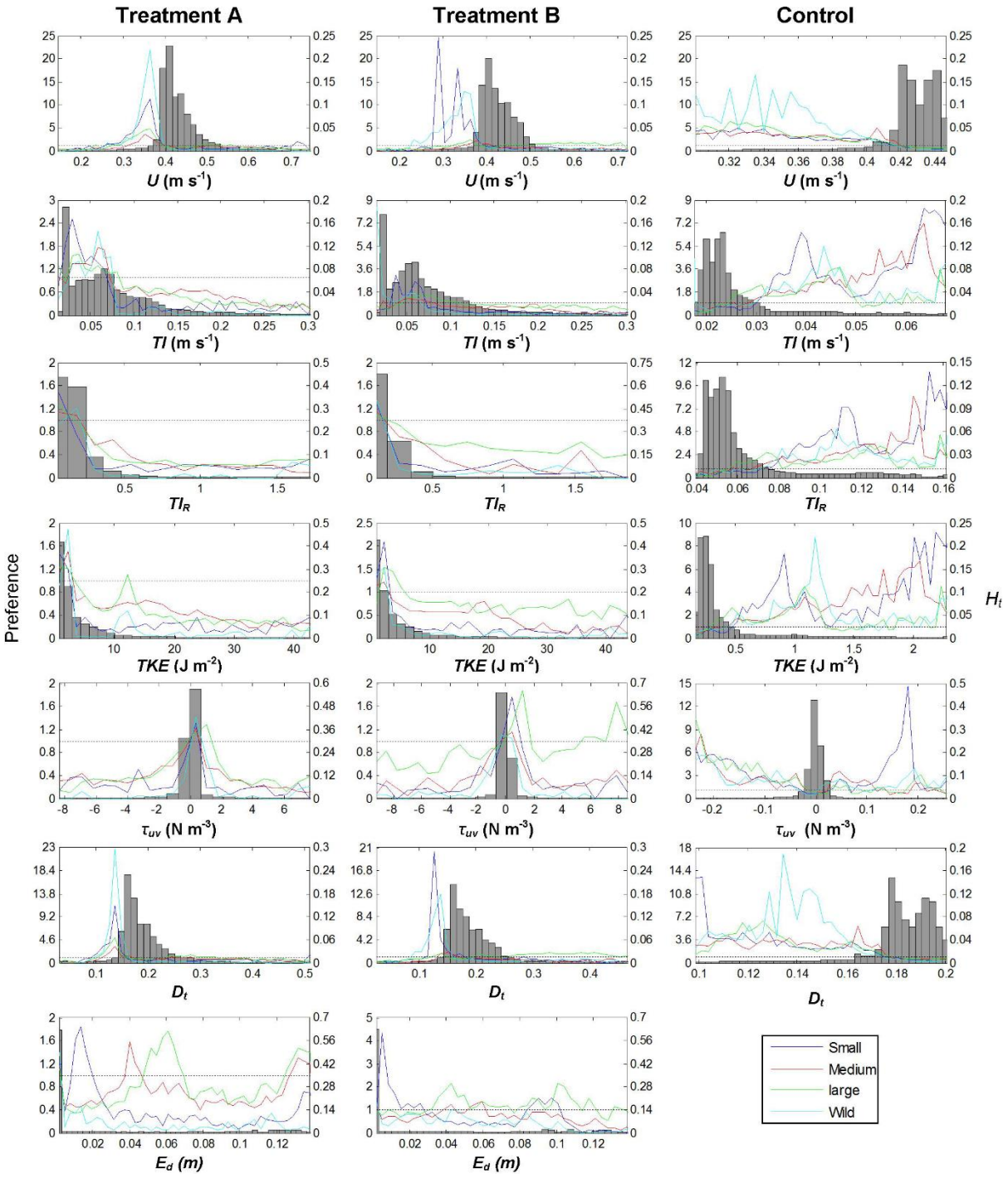

Figure 8. Group preference curves for wild and small, medium and large hatchery brown trout *(Salmo trutta)* under treatment A (n = 3, 11, 12, 13, respectively), B (n = 5, 11, 4, 7, respectively), and the control (n = 3, 8, 3, 4, respectively) for mean velocity (U) (m s^{-1}), turbulence intensity (TI) (m s^{-1}), relative turbulence intensity (TI_R), turbulent kinetic energy (TKE) (J m^{-3}), horizontal Reynolds shear stress (τ_{uv}) (N m^{-2}), drag (D), and eddy diameter (E_d) (m). Left axis is preference curve scale and

right axis is total available hydrodynamic space histogram (H_t) scale (grey bars). Solid grey line is for reference purposes and represents an even distribution (i.e. preference = 1). Note: Axis scales differ between graphs to aid in interpretation.

Table S1 Reynolds number (Re), estimated vortex shedding frequency (f), and wake wavelength (λ) downstream of each cylinder (d) used in an experimental study to investigate space use of brown trout, *Salmo trutta*, in a complex hydrodynamic environment.

d (mm)	Re	f (Hz)	λ (m)
10	2699	13.67	0.03
20	5398	6.83	0.06
30	9097	4.56	0.09
40	10797	3.42	0.12
50	13496	2.73	0.15
60	16195	2.28	0.18
70	18894	1.95	0.21
80	21593	1.71	0.24
90	24292	1.52	0.27

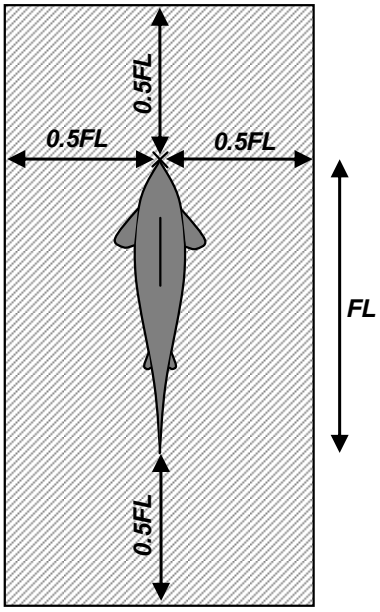

Figure S1 The mechanosensory field of detection (MFoD) allocated to each fish and used to assess the area it sampled during hydrodynamic space use experiments in a large open channel flume.

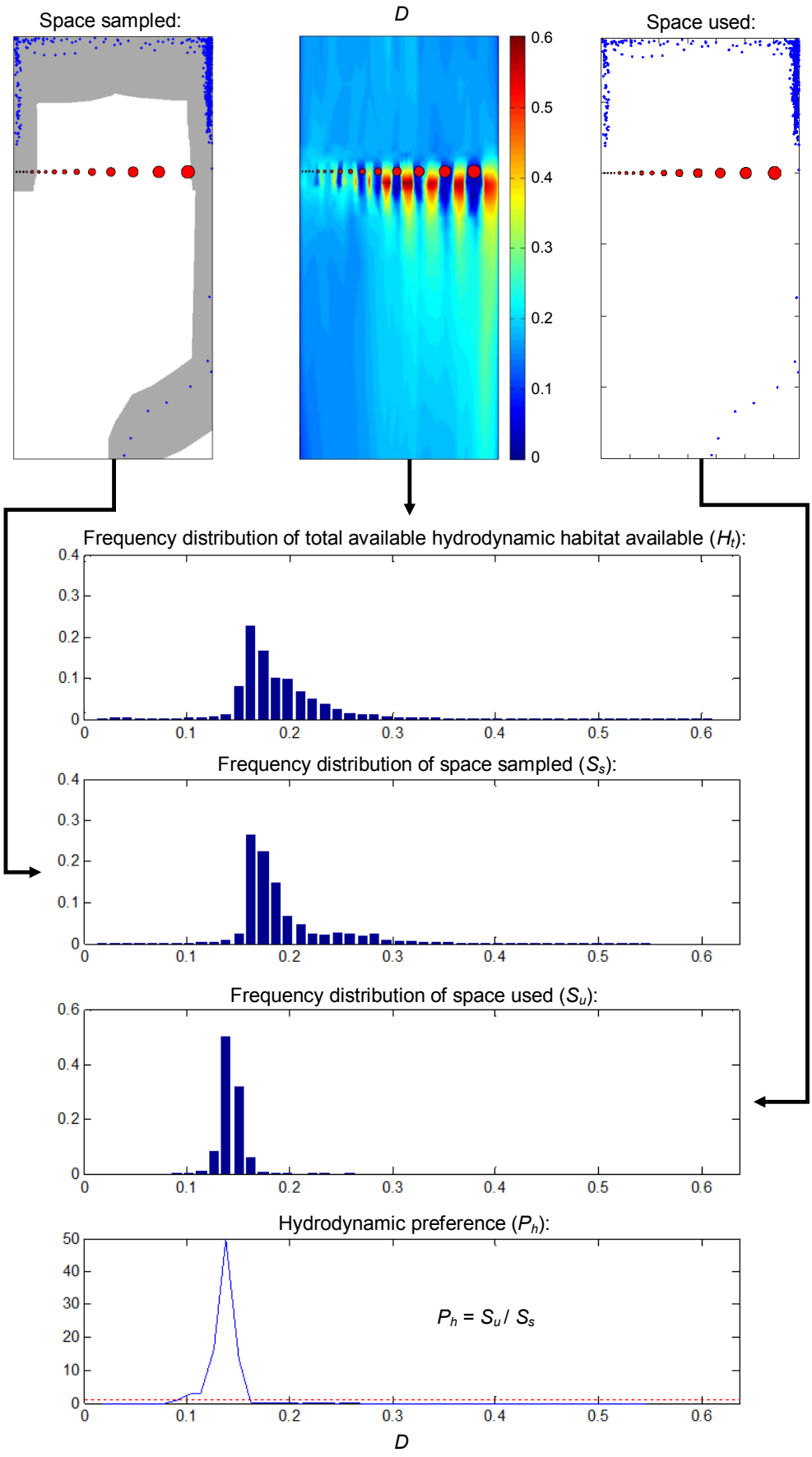

Journal of Experimental Biology • Supplementary information

Figure S2 Schematic representation of how preference was calculated. Example using data for a wild trout (FL: 223 mm) under treatment A (Trial 54, duration: 3600 seconds) for turbulent drag (*D*). Schematic shows plots of the hydrodynamic habitat available (colour intensity plot of *D*) (top middle), the area the fish sampled (grey area) (top left) and space used (blue dots – representing snout position each second) (top right) along with the corresponding frequency distributions of total available (H_t), sampled (S_s) and used (S_u) turbulent drag (*D*) during the trial. The resulting hydrodynamic preference (P_h) for turbulent drag, where $P_h = S_u/S_s$ (calculated for each bin of the S_u and S_s data), is shown in the bottom plot as a solid blue line. The red dashed line in the bottom plot is for reference purposes and represents an even distribution (i.e. preference = 1).

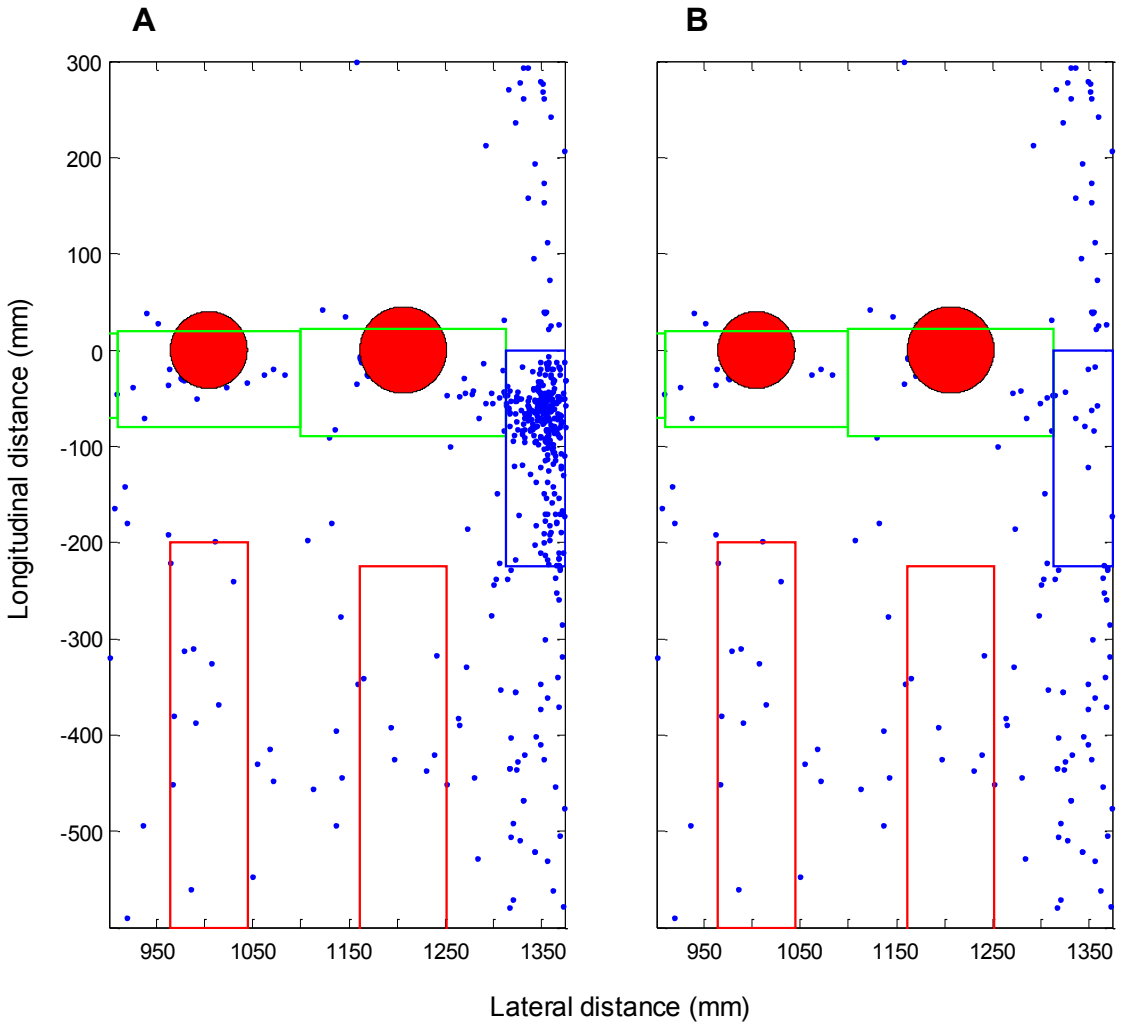

Figure S3 Schematic representation of how excessive use of specialised behavioural zones (SBZs) was accounted for in the data. Example using data for a large hatchery trout (FL: 323 mm) under treatment A (Trial 4, duration: 3600 seconds) with a specific focus on the wall holding SBZ adjacent to the 90 mm cylinder (blue rectangle). A) Raw space use data – 272 instances of the trout being present in the wall holding zone. B) Modified space use data – If distribution had been even then the trout would have only used the zone 12 times. Hence 260 points (272 – 12) from within the SBZ were randomly removed. This was repeated for each SBZ and, therefore, the influence of fish preference for SBZ was removed from the final preference curves.

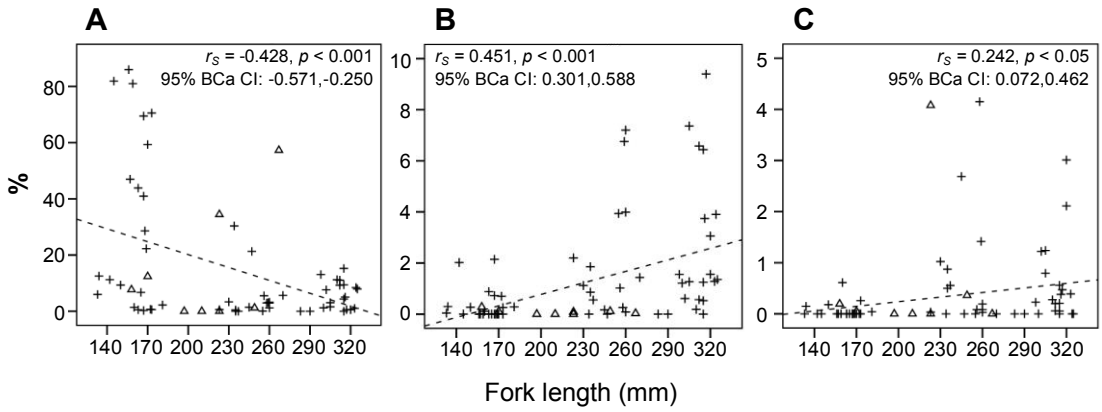

Figure S4. Relationship between percentage of a trial that hatchery (crosses, *n* = 58) and wild (triangles, *n* = 8) trout spent in the tail holding (A), Kármán gaiting (B) and bow riding (C) zones and fork length (FL) (mm) in treatment A and B combined. Dashed line represents the linear correlation. Text is the Pearson's correlation coefficient (r_S) and significance level (p) and the bootstrapped (n=2000) bias corrected and accelerated (BCa) 95% confidence intervals (CI) of r_S.

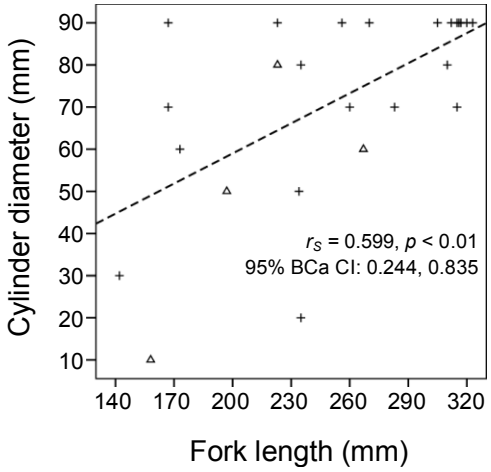

Figure S5. The relationship between trout fork length (mm) and the cylinder diameter (mm) of the entraining zone that hatchery (crosses, n = 21) and wild (triangles, *n* = 4) trout preferentially choose to utilise in treatment A and B combined. Dashed line represents the linear correlation. Text is the Pearson's correlation coefficient (r_S) and significance level (p) and the bootstrapped (n=2000) bias corrected and accelerated (BCa) 95% confidence intervals (CI) of r_S.